Synthesis of Thermally Stable Carboxymethyl Cellulose/Metal Biodegradable Nanocomposite Films for Potential Biological Applications

ARTICLE *in* BIOMACROMOLECULES · JANUARY 2007

Impact Factor: 5.75

2 AUTHORS:

Mallikarjuna N. Nadagouda
United States Environmental Protection Age…
164 PUBLICATIONS **3,965** CITATIONS
SEE PROFILE

Rajender S Varma
United States Environmental Protection Age…
541 PUBLICATIONS **15,514** CITATIONS
SEE PROFILE

Synthesis of Thermally Stable Carboxymethyl Cellulose/Metal Biodegradable Nanocomposites for Potential Biological Applications

Mallikarjuna N. Nadagouda and Rajender S. Varma*

Sustainable Technology Division, U.S. Environmental Protection Agency, National Risk Management Research Laboratory, 26 West Martin Luther King Drive, MS 443, Cincinnati, Ohio 45268

Received April 24, 2007

A green approach is described that generates bulk quantities of nanocomposites containing transition metals such as Cu, Ag, In, and Fe at room temperature using a biodegradable polymer, carboxymethyl cellulose (CMC), by reacting respective metal salts with the sodium salt of CMC in aqueous media. These nanocomposites exhibit broader decomposition temperatures when compared with control CMC, and Ag-based CMC nanocomposites exhibit a luminescent property at longer wavelengths. The noble metals such as Au, Pt, and Pd do not react at room temperature with aqueous solutions of CMC, but do so rapidly under microwave irradiation (MW) conditions at 100 °C. This environmentally benign approach, which provides facile entry to the production of multiple shaped noble nanostructures without using any toxic reducing agent such as sodium borohydride ($NaBH_4$), hydroxylamine hydrochloride, and so forth, and/or a capping/surfactant agent, and which uses a benign biodegradable polymer CMC, could find widespread technological and medicinal applications. The ensuing nanocomposites derived at room temperature and MW conditions were characterized using scanning electron microscopy, transmission electron microscopy, infrared spectroscopy, UV−visible spectroscopy, X-ray mapping, energy-dispersive analysis, and thermogravimetric analysis.

Introduction

Metal-containing composite materials that exhibit antimicrobial properties are promising for biotechnological applications, such as safe food packaging or sterile coatings for biomedical devices.[1] Recently there has been a lot of developmental work on biodegradable and copper-based nanocomposite materials[2−5] with focus on their antimicrobial properties.[6] The antibacterial properties of composites, mainly bearing silver, have been studied;[6−10] they exert a stronger toxic action against bacteria compared to other organisms varying from fungi to humans.[11,12] Eukaryotes such as fungi can be dangerous pathogenic agents, and effective antifungal aqueous solutions based on copper ions[13] as well as complex copper species[14−17] or copper-containing polymers[18,19] have often been proposed and used. There have been reports on the antimicrobial properties of technologically appealing materials such as fabrics, paints, or coatings containing copper-based active powders or pigments,[20−22] leading to the exploration of copper, silver, and other noble metal-based composites for effective biological applications.

Nanocomposites of cellulose and its derivatives are gaining importance because of their value-added applications in science and technology,[23] for example, in nanocomposites of cellulose-based electrolytes,[24] high-performance composite materials,[25] organoclay-exfoliated cellulose with improved mechanical properties,[26] nanocomposites with good tensile strength,[27] biomedical applications,[28] and as host materials.[29] Consequently, present innovations are more focused on understanding the structure−property relationships and adaptation of these cellulose-derived products for specific newer applications that result in decreased use of chemicals. Among cellulosic ethers, carboxymethyl celluloses (CMCs) are very important derivatives of cellulose; they have good solubility, high chemical stability, and are toxicologically innocuous. They are processed in a dissolved or highly swollen state[23] and are dominant polymers in numerous industrial applications, especially where consistency in the quality of aqueous media and water-containing systems is required.

Petridis et al. reported that dropwise addition of CMC solution to a Cu or Fe salt in *n*-butanol leads to self-assembled, permeable, millimeter-sized metal-ion-derivatized CMC hollow capsules.[30] Herein, we report a simple and convenient approach that generates nanocomposites at room temperature in aqueous medium, encompassing various metal salts such as Cu, In, Fe, and Ag, and these materials may find potential applications such as in antibacterial, antifungal coatings, food packaging, and biomedical devices.

In contrast, CMC does not produce nanocomposites when reacted with noble metal salts such as Au, Pt, and Pd under aqueous conditions at room temperature. However, reduction can be accomplished in these systems by reacting CMC aqueous solution with noble metal salts under microwave (MW) irradiation conditions at 100 °C, where CMC acts as a capping and reducing agent. MW irradiation provides rapid and uniform heating of reagents, solvents, and intermediates,[31−34] and this homogeneous heating also provides uniform nucleation and growth conditions, resulting in the formation of homogeneous nanomaterials with smaller sizes. Power dissipation is fairly uniform throughout with "deep" inside-out heating of the solvent, which leads to better crystallinity, and pioneering work has been recently conducted involving various process intensifications and novel polymer syntheses.[35−37] This environmentally benign method is a one-pot procedure that provides facile entry to the production of multiple shaped noble nanostructures

* Corresponding author. Tel: (513) 487-2701. Fax: (513) 569-7677. E-mail: varma.rajender@epa.gov.

10.1021/bm700446p CCC: $37.00
Published on Web 08/01/2007

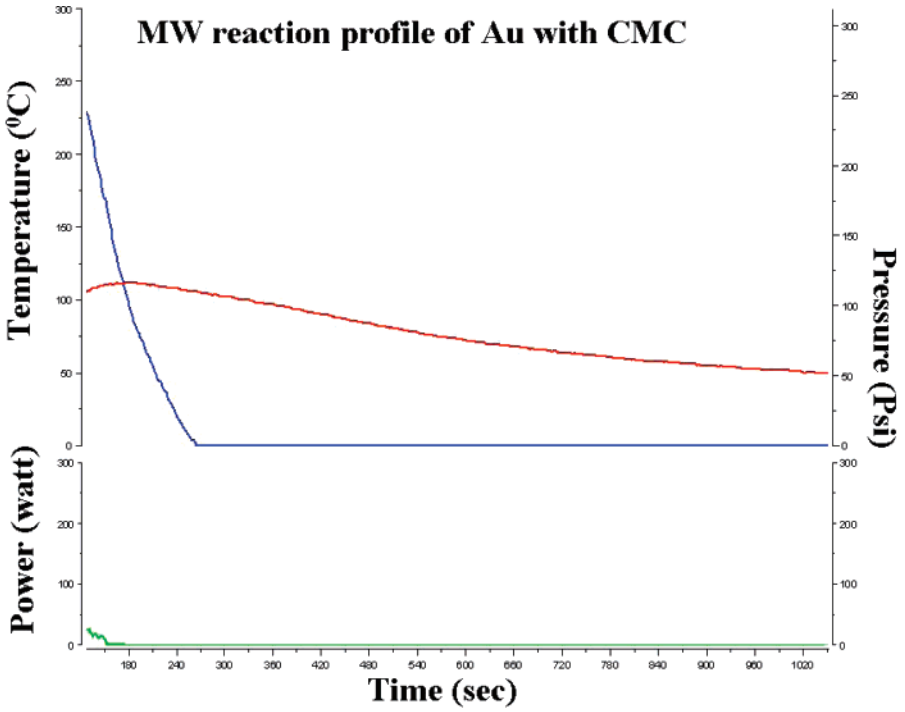

Figure 1. Typical reaction profile of Au with CMC under MW irradiation at 100 °C.

without using any reducing agent and/or capping/surfactant agent and uses a benign biodegradable polymer CMC, which could find a host of technological and medicinal applications.

Experimental Section

All of the chemical reagents used in this study were of analytical grade and used without any further purification. The reactants used were Na_2PtCl_6 $6H_2O$ (99.99%, Acros), $CuCl_2$ (99.9%, Aldrich), $InCl_3$ (99.99%, Aldrich), $HAuCl_4$ $3H_2O$ (99.99%, Acros), $Fe(NO_3)_3$ (98%, Aldrich), $AgNO_3$ (99.99%, Aldrich), $PdCl_2$ (99.99%, Acros), and CMC ($M_w \sim 90\,000$, Aldrich).

The fabrication of a representative CMC-embedded Cu nanocomposite was accomplished as follows: An aqueous solution of 0.1 M $CuCl_2 \cdot 2H_2O$ (4 mL, 0.1 N) was added to an aqueous sodium CMC solution (4 mL, 3 wt %) at room temperature in a 10 mL test tube. Similarly, separate experiments were conducted with 0.1 M $FeCl_3 \cdot 6H_2O$, 0.1 N $InCl_3$, and 0.1 $AgNO_3$ at room temperature (Figure S1, Supporting Information). The reactions were complete within a few seconds, and the film formation, that is, coloration, depends on the metal salt used for the preparation with CMC. In the case of 0.01 N $HAuCl_4$, 0.01 N Na_2PtCl_6, and 0.01 N $PdCl_2$, the reaction mixture was irradiated with microwaves at 100 °C for 5 min; the heating profile of Au with CMC is shown in Figure 1, and the product photograph is shown in Figure S2 (Supporting Information). Microwave heating experiments were conducted using a CEM Discover microwave reactor. Transmission electron micrographs (TEM) were obtained from a JEOL JSM-1200 II microscope at an operating voltage of 120 kV. For TEM sample preparation, the solids were dispersed in water and sonicated for 30 min, and then a drop of dispersed particles was cast onto a copper grid and dried at room temperature. Scanning electron micrographs (SEM) were obtained from a JEOL-6400 microscope. For SEM micrographs, powder samples were placed on a carbon tape, and micrographs were recorded. The operating voltage for SEM was maintained at 20 k. Thermogravimetric analysis (TGA) curves were obtained using a Perkin-Elmer thermal analyzer with a heating rate of 10 °C/min under air.

Results and Discussion

The addition of metal salts such as Cu, Fe, In, and Ag to an aqueous solution of CMC led to the formation of metal-coordinated CMC nanocomposites. The specific reaction between metal and CMC is just metal displacement reaction. The Na^+ ion from the CMC is replaced with the respective metal salt, and the soluble byproduct, NaCl, dissolves (see eq 1). However, this reaction is feasible only for transition metals; noble metals such as Au, Pd, and Pt do not readily undergo a metal displacement reaction with the Na^+ ion. The chelating effect of carboxyl groups probably plays an important role in the formation of complexes with various metal ions. At room temperature, noble metals do not chelate with carboxyl groups. However, they undergo reduction with CMC at higher temperatures (100 °C) under MW irradiation. The possible reduction entails the coupling of polar hydroxyl units in β-glucopyranose units with microwaves, which reduce metal ions. The color formation of CMC nanocomposites depended on the metal salt used for the preparation: Cu, blue; In, milky white; Fe, brown; and Ag, light yellow (Figure S1). A typical reaction profile and photographic image of Au with CMC under MW irradiation at 100 °C is shown in Figures 1 and S2 (Supporting Information), respectively. The control experiments were conducted in oil bath at 100 °C under similar conditions. The reduction of Au nanoparticles with CMC occurs within 5−6 min, whereas Pd takes more than 2 h, and Pt does not undergo reduction even after 2 h.

$$ROCH_2COONa + MCl \rightarrow ROCH_2COOAu + NaCl \quad (R = \text{cello-biose units, M = metal ion}) \quad (1)$$

The formation of noble nanometals was confirmed using UV spectroscopy (Figure 2). Gold nanoparticles exhibited an intense peak at 517 nm, and continuous absorption in the UV range was observed for Pt and Pd nanostructures, as expected (Figure 2). In order to study the metal dispersion in CMC, we recorded the X-ray mapping images using SEM (Figure 3). Metals such as Cu, In, Fe, and Ag were dispersed uniformly throughout the CMC matrix, and there were no agglomerations observed. In the X-ray mapping images, red spots correspond to metals, and green areas correspond to the carbon backbone of CMC. The energy-dispersive X-ray analyses (EDX) of Cu, In, Fe, and Ag are shown in the insets of Figure 3a−d, respectively.

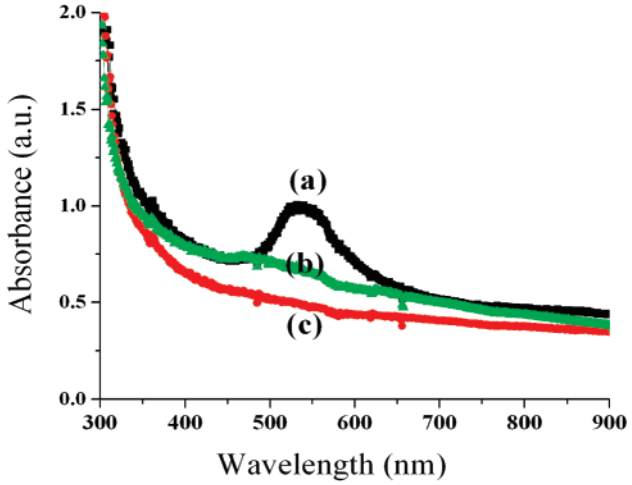

Figure 2. UV spectra of CMC-reduced (a) Au, (b) Pt, and (c) Pd synthesized using MW irradiation for 5 min at 100 °C.

Nanocomposites embedded with Cu form aligned structures (Figures S3a and S4, Supporting Information). This trend continues for In and Ag with slightly distorted structures (see Figure S3c,d, Supporting Information). However, Fe-embedded nanocomposites do not form aligned structures (Figure S3b, Supporting Information).

IR spectroscopy is an important tool that determines the coordination property of a ligand or polymer with any metal. In order to understand the metal chelation with the carboxyl group of CMC, we recorded IR spectra for the nanocomposites (Figure 4). The IR spectra of all the CMC nanocomposites containing Cu, Fe, and In synthesized at room temperature in aqueous media show the typical absorptions of the cellulose backbone as well as the presence of a carboxyl methyl ether group at 1605 cm^{-1} (Figure 4). It is evident that the broad absorption band at 3432 cm^{-1} is due to the stretching frequency of the −OH group[38,39] as well as intramolecular and intermolecular hydrogen bonds. The bands at 2920 cm^{-1} are due to C−H stretching vibration. The bands around 1420 and 1320 cm^{-1} are assigned to $-CH_2$ scissoring and −OH bending vibration, respectively. The bands at 1060 cm^{-1} are due to $-CH-O-CH_2$ stretching.[38,39]

The spectrum of native CMC is also shown in Figure 4. Clearly, all nanocomposites have the typical absorption band characteristics described earlier for CMC nanocomposites, namely, an −OH group (3432 cm^{-1}); C−H stretching (2920 cm^{-1}); $-CH_2$ scissoring and −OH bending (1420 and 1320 cm^{-1}); and $-CH-O-CH_2$ stretching (1060 cm^{-1}).[26,27] Consequently, no major changes were observed in IR frequency when compared with that of pure CMC, suggesting that the reaction between metal salts and CMC is a simple metal displacement reaction. Similarly, CMC-reduced nanostructures of (a) Au, (b) Pt, and (c) Pd synthesized using MW irradiation for 5 min at 100 °C show no major changes when compared to native CMC (Figure 5).

It is interesting to note that Cu metal displacement reactions with sodium salt afforded needle-like nanostructures in the form of bushes that are well dispersed in the CMC matrix, as shown in TEM images (Figure 6a), whereas In and Fe formed spherical nanoparticles uniformly embedded in the CMC matrix (Figure 6b,c). On the other hand, Ag crystallized in spherical nanoparticles along with majority of cube-shaped particles (Figure 6d). Figure 7 shows the corresponding electron diffraction pattern for Cu-, In-, and Ag-embedded nanocomposites. Cu, In, and Ag crystallized in cubic symmetry. However, in the case of Cu, we also observed diffraction planes corresponding to the $Cu-(OH)_2$ face.

The diffraction rings in Figure 7c could be indexed on the basis of the face-centered cubic (fcc) structure of silver. The reduction of noble metals in the presence of MW irradiation yielded irregularly shaped nanoparticles (see Figures 8a,b and S5−S7 (Supporting Information) for TEM and selected area electron diffraction (SAED) images). Figure 8c shows the SAED pattern for Au individual nanoparticles by directing the electron

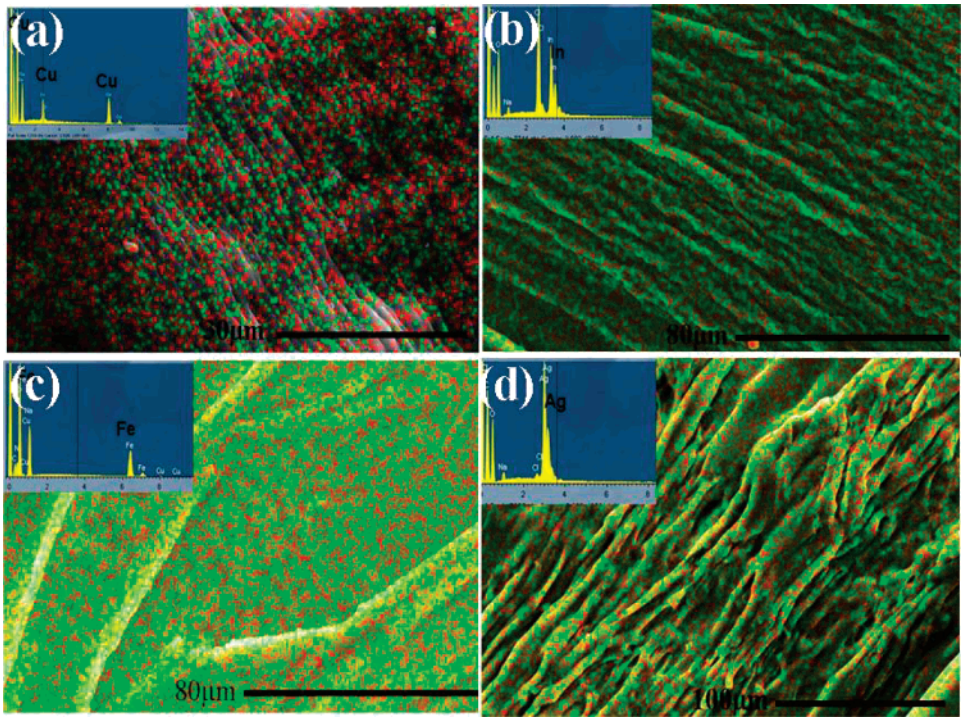

Figure 3. SEM image of CMC nanocomposites with (a) Cu, (b) In, (c) Fe, and (d) Ag. Red spotted area corresponds to metal, and green area represents carbon. Inset corresponds to their respective EDX.

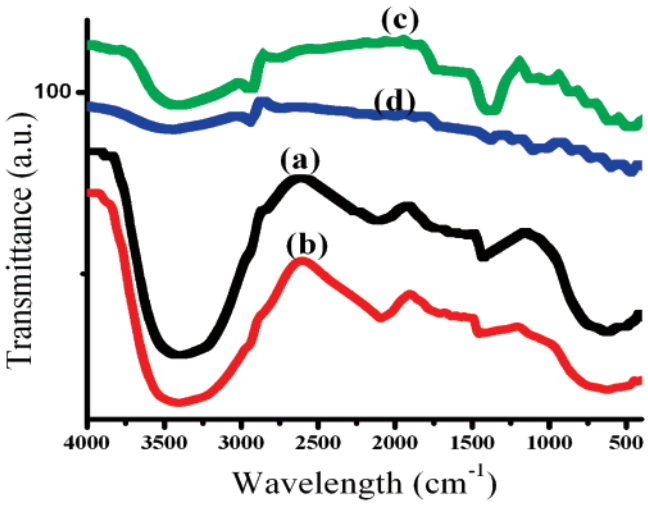

Figure 4. IR spectra of CMC nanocomposites with (a) Cu, (b) In, (c) Fe, and (d) control CMC synthesized at room temperature.

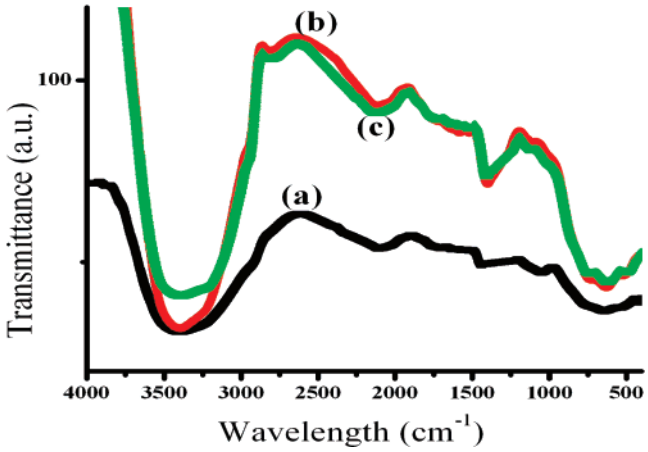

Figure 5. IR spectra of CMC-reduced nanostructures of (a) Au, (b) Pt, and (c) Pd synthesized using MW irradiation for 5 min at 100 °C.

beam perpendicular to one of its faces, indicating that each nanoparticle was a single crystal.

Three sets of spots could be identified based on their *d*-spacing: The strongest spots could be indexed to the {220} reflection of fcc gold. The outer set corresponded to the {422} Bragg reflections. These two sets of reflections were both allowed by a fcc lattice. The third set with very weak spots could be indexed to (1/3){422} reflection, which is normally forbidden by an fcc lattice. Similarly, Pd also crystallizes in cubic symmetry (Figure 8d).

In order to understand the thermal stability of nanocomposites, a TGA of CMC containing In, Cu, Fe, and Ag was conducted, and the thermograms are shown in Figure 9. Irrespective of the metal used to complex with CMC, all the nanocomposite materials had broader decomposition temperatures when compared to that of the control CMC sample. However, these broad decomposition temperatures, that is, thermal stability, vary depending upon the metal salt used for the preparation. The possible reason is that different metals have different coordinating capacity with the chelating agent, that is, the carboxyl group of CMC. For example, Cu− and In−CMC nanocomposites start degrading at ~200 °C with broader decomposition temperatures when compared with those of Fe− and Ag−CMC nanocomposites (Figure 9a). The control sample of native CMC experienced a 50 wt % loss at a temperature of ~290 °C (Figure 10), and it is a very steep curve, whereas CMC nanocomposites experienced a 50 wt % loss at a temperature of around 400 °C (Figure 9).

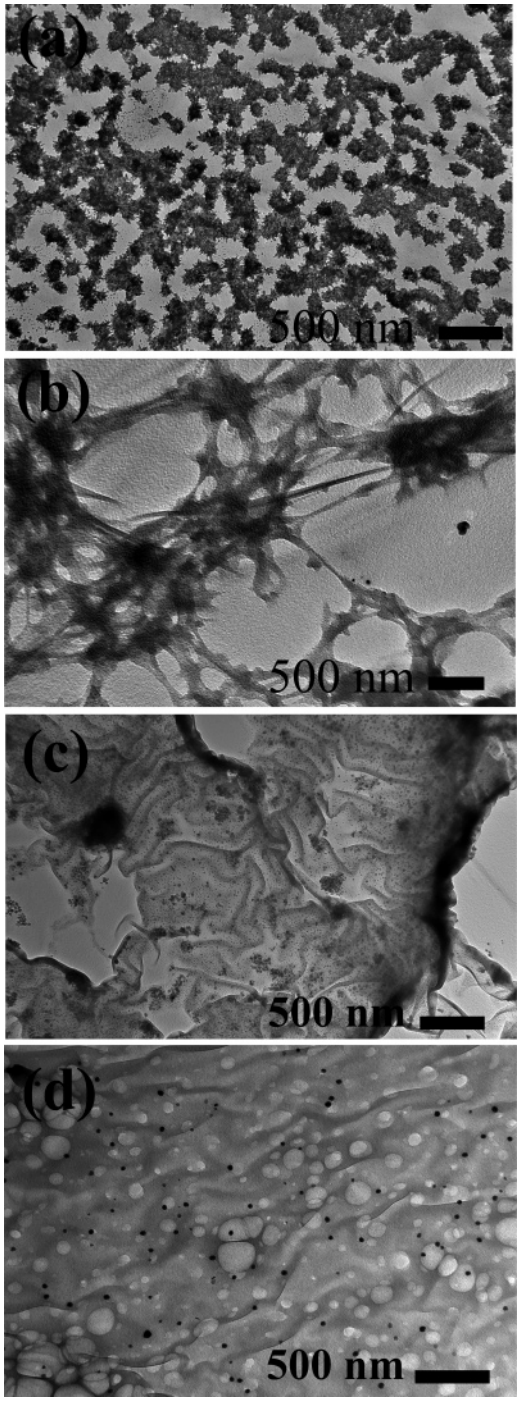

Figure 6. TEM images of CMC nanocomposites with (a) Cu, (b) In, (c) Fe, and (d) Ag.

These nanocomposites and reduced noble metals in the CMC matrix may find a wide range of technological and biological applications. For example, Ag-based CMC nanocomposites exhibited luminescent properties (Figure 11) and could be used in biolabeling for ultrasensitive detection of biological species such as antibodies, DNA, and cells, thus replacing other toxic semiconducting nanoparticle-based biolabeling methods, which normally use CdS−Mn/ZnS.[40,41] Nanocomposite labels have many advantages over organic fluorescent labels, such as their high sensitivity, low toxicity, and large Stokes' shift; therefore they have become more and more popular in various biological

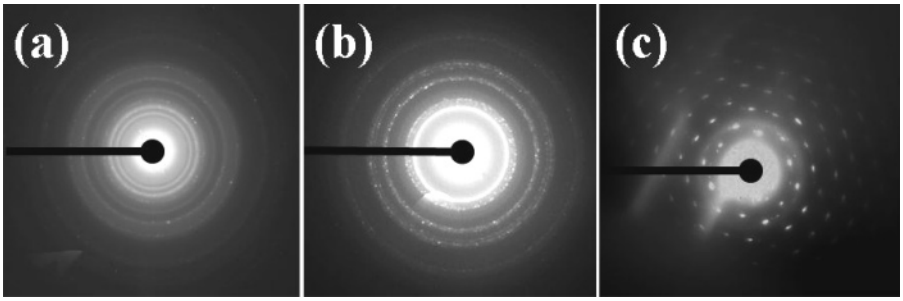

Figure 7. SAED pattern of CMC nanocomposite film with (a) Cu, (b) In, and (c) Ag.

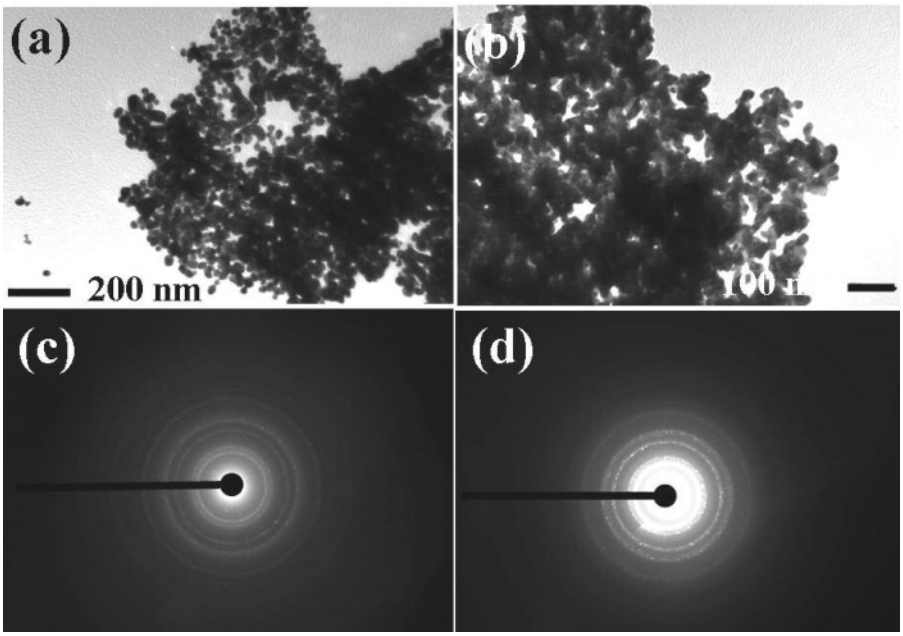

Figure 8. TEM images of CMC-reduced (a) Au and (b) Pd, and SAED pattern of (c) Au and (d) Pd nanostructures.

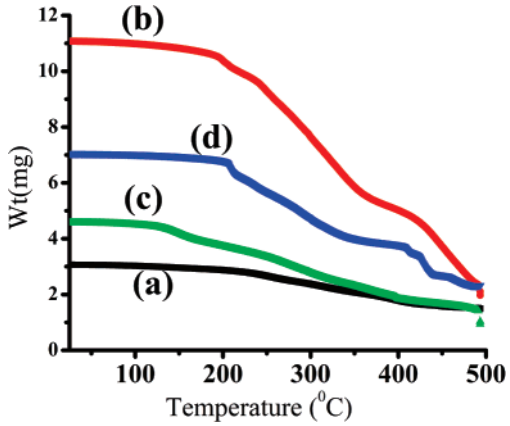

Figure 9. TGA thermograms of CMC nanocomposites with (a) In, (b) Cu, (c) Fe, and (d) Ag.

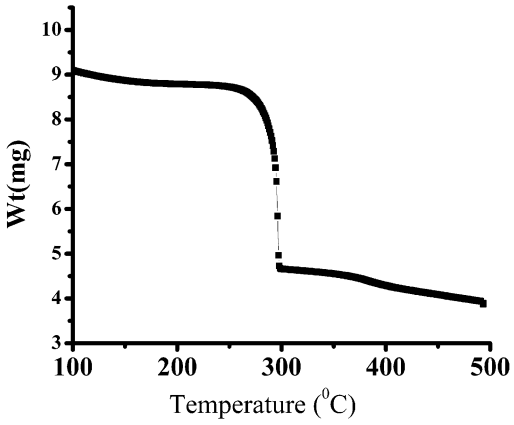

Figure 10. TGA thermogram of control CMC.

applications. Nanocomposites derived from biodegradable cellulose with Cu, Ag, Fe, and In metals may find potential applications such as in antibacterial, antifungal coatings, food packaging, and biomedical devices.

Conclusions

In summary, we describe (i) the synthesis of nanocomposites of CMC with Cu, In, Fe, and Ag at room temperature; (ii) a convenient method to obtain nanocomposites of Cu, In, Fe, and Ag, which have better thermal properties (thermal stability) and broader decomposition temperatures when compared with those of pure CMC; (iii) the spontaneous reduction of noble metals such as Au, Pt, and Pd that can be accomplished using CMC under MW irradiation at 100 °C within 5 min without using any reducing or surfactant agents; (iv) Ag-based CMC nanocomposite materials that exhibit luminescent properties and could be used in biolabeling for ultrasensitive detection of biological species such as antibodies, DNA, and cells, thus replacing other toxic semiconducting nanoparticles-based biolabeling; and (v) the idea that these nanocomposites derived from biodegradable cellulose with Cu, Ag, Fe, In, and noble metals may find potential applications such as in antibacterial, antifungal coatings, food packaging, and biomedical devices.

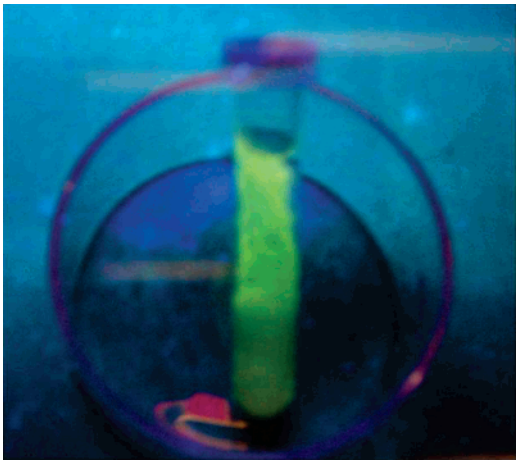

Figure 11. Fluorescence image of green light-emitting Ag−CMC nanocomposite film under a 365-nm multiband UV source.

Acknowledgment. M.N.N. was supported, in part, by the Postgraduate Research Program at the National Risk Management Research Laboratory administered by the Oak Ridge Institute for Science and Education through an interagency agreement between the U.S. Department of Energy and the U.S. Environmental Protection Agency. M.N.N. is thankful to Cristina Bennet-Stamper for TEM alignment.

Supporting Information Available. Additional SEM, TEM, and SAED images. This material is available free of charge via the Internet at http://pubs.acs.org.

References and Notes

(1) Klabunde, K. J. *Nanoscale Materials in Chemistry*; Kenneth, J. K., Ed.; Wiley-Interscience: New York, 2001.
(2) Zaporojtchenko, V.; Strunskus, T.; Erichsen, J.; Faupel, F. *Macromolecules* **2001**, *34*, 1125−1127.
(3) Luckarift, H. R.; Dickerson, M. B.; Sandhage, H. K.; Spain, J. C. *Small* **2006**, *2*, 640−643.
(4) Wang, X.; Du, Y.; Yang, J.; Wang, X.; Shi, X.; Hu, Y. *Polymer* **2006**, *47*, 6738−6744.
(5) Gubin, S. P. *Colloids Surf.* **2002**, *A 202*, 155−163.
(6) Balog, L.; Swason, D. R.; Tomalia, D. A.; Hagnauer, G. L.; McManus, A. T. *Nano Lett.* **2001**, *1*, 18−21.
(7) Kasuga, T.; Hume, H.; Abe, Y. *J. Am. Ceram. Soc.* **1997**, *80*, 777−780.
(8) Kasuga, T.; Nogami, M.; Abe, Y. *J. Am. Ceram. Soc.* **1999**, *82*, 765−767.
(9) Yang, M. R.; Chen, K. S.; Tsai, J. C.; Tseng, C. C.; Lin, S. F. *Mater. Sci. Eng.* **2002**, *C20*, 167−173.
(10) Kwak, S. Y.; Kim, S. H.; Kim, S. S. *Environ. Sci. Technol.* **2001**, *35*, 2388−2394.
(11) Kierans, M.; Staines, A. M.; Bennet, H.; Gadd, G. M. *Biol. Met.* **1991**, *4*, 100−106.
(12) Ciriolo, M. R.; Civitareale, P.; Carri, M. T.; De Martino, A.; Galiazzo, F.; Rotilio, G. *J. Biol. Chem.* **1994**, *269*, 25783−25794.
(13) Avery, S. V.; Howlett, N. G.; Radice, S. *Appl. Environ. Microbiol.* **1996**, *62*, 3960−3966.
(14) Zoruddu, M. A.; Zanetti, S.; Pogni, R.; Basosi, R. *J. Inorg. Biochem.* **1996**, *63*, 291−300.
(15) Esteban-Cubillo, A.; Pecharromán, C.; Aguilar, E.; Santarén, J.; Moya, J. S. *J. Mater. Sci.* **2006**, *41*, 5208−5212.
(16) Ali, M. A.; Mirza, A. H.; Hossain, A. M. S.; Nazimuddin, M. *Polyhedron* **2001**, *20*, 1045−1052.
(17) Belicchi Ferrari, M.; Bisceglie, F.; Gasparri Fava, G.; Pelosi, G.; Tarasconi Albertini, R.; Pinelli, S. *J. Inorg. Biochem.* **2002**, *89*, 36−44.
(18) Ooiso, Y. Jpn. Kokai Tokkyo Koho, Patent Nos. JP 08333213, JP 08333261, 1996.
(19) Borkow, G.; Gabbay, J. *FASEB J.* **2004**, *18*, 1728−1730.
(20) Park, J. S.; Kim, J. H.; Nho, Y. C.; Kwon, O. H. *J. Appl. Polym. Sci.* **1998**, *69*, 2213−2220.
(21) Narita, T. Jpn. Kokai Tokkyo Koho, Patent No. JP 2000026221, 2000.
(22) Saita, J.; Sugita, S.; Kojima, K.; Nakamura, H.; Takashima, T. Jpn. Kokai Tokkyo Koho, Patent No. JP 10158539, 1998.
(23) Klemm, D.; Heublein, B.; Fink, H.; Bohn, A. *Angew. Chem., Int. Ed.* **2005**, *44*, 2−37.
(24) Samir, M. A. S. A.; Alloin, F.; Gorecki, W.; Sanchez, J.; Dufresne, A. *J. Phys. Chem. B* **2004**, *108*, 10845−10852. Cranston, E. D.; Gray, D. G. *Biomacromolecules* **2006**, *7*, 2522−2530.
(25) Kohler, R.; Nebel, K. *Macromol. Symp.* **2006**, *244*, 97−106.
(26) Park, H.; Liang, X.; Mohanty, A. K.; Misra, M.; Drzal, L. T. *Macromolecules* **2004**, *37*, 9076−9082.
(27) Ruan, D.; Zhang, L.; Zhang, Z.; Xia, X. *J. Polym. Sci. Part B: Polym. Phys.* **2004**, *42*, 367−373.
(28) Czaja, W. K.; Young, D. J.; Kawecki, M.; Brown, R. M., Jr. *Biomacromolecules* **2007**, *8*, 1−12.
(29) Ruan, D.; Huang, Q.; Zhang, L. *Macromol. Mater. Eng.* **2005**, *290*, 1017−1024.
(30) Bourlinos, A. B.; Petridis, D. *Chem. Commun.* **2002**, 2788−2789.
(31) Varma, R. S. Microwave Technology−Chemical Synthesis Applications. In *Kirk−Othmer Encyclopedia of Chemical Technology*, 5th ed.; John Wiley & Sons: Hoboken, NJ, 2006; Vol. 16; pp 538−594.
(32) Varma, R. S. *Advances in Green Chemistry: Chemical Syntheses Using Microwave Irradiation*; AstraZeneca Research Foundation India: Bangalore, India, 2002.
(33) Varma, R. S. In *Microwaves in Organic Synthesis*; Loupy, A., Ed.; Wiley-VCH: Weinheim, Germany, 2006; pp 362−415.
(34) Nadagouda, M. N.; Varma, R. S. *Cryst. Growth Des.* **2007**, *7*, 686−690.
(35) Galbrecht, F.; Bünnagel, T. W.; Scherf, U.; Farrell, T. *Macromol. Rapid Commun.* **2007**, *28*, 387−394.
(36) Hoogenboom, R.; Schubert, U. S. *Macromol. Rapid Commun.* **2007**, *28*, 368−386.
(37) Glasnov, T. N.; Kappe, C. O. *Macromol. Rapid Commun.* **2007**, *28*, 395−410.
(38) Kondo, T. *Cellulose* **1997**, *4*, 281−292.
(39) Biswal, D. R.; Singh, R. P. *Carbohydr. Polym.* **2004**, *57*, 379−387.
(40) Santra, S.; Yang, H.; Holloway, P. H.; Stanley, J. T.; Mericle, R. A. *J. Am. Chem. Soc.* **2005**, *127*, 1656−1657.
(41) Nagasaki, Y.; Ishii, T.; Sunaga, Y.; Watanabe, Y.; Otsuka, H.; Kataoka, K. *Langmuir* **2004**, *20*, 6396−6400.

BM700446P